Three Dimensional Mhd Flow Of A Casson Fluid Over A Permeable Axisymmetric Shrinking Sheet With Heat Generation Or Absorption And Slip Velocity

P. Sathies Kumar[1] and K. Gangadhar[2]

[1]Department of Mathematics, Raghava Degree College, Ongole, A.P
[2]Department of Mathematics, AcharyaNagarjuna Universityongole campus, Ongole, Andhra Pradesh -523001, India

Abstract*: This paper investigated the effects of partial slip, viscous dissipation, heat generation or absorption and convective boundary condition on three dimensional magnetohydrodynamic flow of Casson fluid and heat and mass transfer past a permeable sheet which shrinks axisymmetrically in its own plate. The governing equations are transformed into a system of non linear ordinary differential equations by using the similarity transformations. The reduced systems of equations are solved by using the fourth order Runge-Kutta Gill procedure together with shooting technique. The results are presented graphically and in tabular form for various controlling parameters. The numerical results are validated by comparisons with previously published results in the literature.*
Keywords: *Casson fluid, MHD, slip velocity, heat and mass transfer,convective boundary condition, heat generation or absorption.*

I.   Introduction

Magneto-hydrodynamic (MHD) boundary layers with heat and mass transfer over flat surfaces are found in many engineering and geophysical applications such as geothermal reservoirs, thermal insulation, enhanced oil recovery, packed-bed catalytic reactors, cooling of nuclear reactors. Many chemical engineering processes like metallurgical and polymer extrusion processes involve cooling of a molten liquid being stretched into a cooling system. The fluid mechanical properties of the penultimate product depend mainly on the cooling liquid used and the rate of stretching. Some polymer liquids like polyethylene oxide and polyisobutylene solution in cetane, having better electromagnetic properties are normally used as cooling liquid as their flow can be regulated by external magnetic fields in order to improve the quality of the final product.Jat and Jhankal(2003) concluded that the skin-friction coefficient increases with increasing the values of Reynolds number and magnetic parameter up to a certain value of Reynolds number and after words it decreases with the increasing values of these parameters and also the heat transfer rate increases with the increasing the values of these parameters. Hayat and Nawaz (2010) studied the effect of MHD on three dimensional flow of a second grade fluid with heat transfer and they concluded that dimensionless tangential velocity $f'(\eta)$ is a decreasing function of magnetic field where as dimensionless lateral velocity $g(\eta)$ increases by increasing magnetic parameter.Turkyilmazoglu (2012) studied the three dimensional MHD laminar stagnation point flow of an electrically conducting fluid on radially stretchable rotating disk in the presence of a uniform vertical magnetic field. Hayat et al.(2013) studied the three dimensional flow of MHD Eyring-Power fluid with Radiation effect and then concluded that magnetic field cause a decrease in the magnitude of velocity components $f'(\eta)$ and $g'(\eta)$.Kar et al. (2013) investigated the effects of MHD, heat source and chemical reaction in a vertical channel through a porous medium.Rajagopal and Pravin(2013) concluded that the surface shear stress in x and y directions and the surface heat transfer and surface mass transfer increase with the magnetic parameter.El-Dabe et al. (2015) concluded that the velocity distribution decreases with increasing the values of magnetic parameter while it increases the values of Casson fluid parameter. Ramzan(2015) discuss the influence of Newtonian heating, viscous dissipation and joule heating on the magneto hydro dynamic (MHD) three dimensional couple stress nanofluid past a stretching surface. Gireesha et al. (2015) investigated MHD boundary layer three dimensional flow and heat transfer of Eyring-Powell fluid towards a linearly stretching sheet in the presence of nanoparticle.

The boundary layer flows of non-Newtonian fluids over a stretching sheet with heat and mass transfer are important in several areas such as extrusion process, glass fibber, paper production, hot rolling, wire drawing, electronic chips, crystal growing, plastic manufactures, and application of paints, food processing and movement of biological fluids (Hayat and Qasim (2011)). Bhargava et al. (2007) discussed heat and mass transfer of boundary layer flow over a nonlinear stretching sheet under the effects of different physical parameters. Khan and Pop (2010) investigated the laminar fluid flow of a nanofluid from the stretching flat

surface by incorporating the effects of Brownian motion, thermophoresis and reported to be the pioneer for this study of stretching sheet in nanofluid. Pal and Mondal (2010) examined the heat and mass transfer over a stretching sheet by considering the effects of buoyancy and solutal buoyancy parameters. Anwar et al. (2012) studied the conjugate effects of heat and mass transfer of nanofluids over a nonlinear stretching sheet.Sumalatha and Shankar (2015) concluded that on increasing the Casson fluid parameter (β), the momentum boundary layer thickness decrease but thermal boundary layer thickness increase. Pramanik(2014) concluded that the increasing the values of Casson parameter is seen to suppress the velocity, temperature is enhance with increasing the Casson parameter. Megahed (2015) studied the effects of internal heat generation or absorption and thermal radiation on MHD viscous Casson fluid flow and heat transfer with second order slip velocity and thermal slip over a permeability sheet and he concluded that increasing the velocity and thermal slip parameters makes a rate of heat transfer decreased. Kameswaran et al. (2014) studied the dual solutions of Casson fluid flow over a stretching or shrinking sheet.

The heat source/sink effects in thermal convection, are significant where there may exist a high temperature differences between the surface (e.g. space craft body) and the ambient fluid. Heat generation is also important in the context of exothermic or endothermic chemical reactions. Raju et al.(2015) investigated the effect of space and temperature dependent heat generation or absorption on three-dimensional magneto hydro dynamic nanofluid flow over a non linearly permeable stretching sheet by using bvp 4c matlab package.Sarojamma and Vendabai (2015) concluded that increasing values of the spatial dependent internal heat generation (A*) as well as temperature dependent internal heat generation (B*) results in the enhancement of temperature.

This paper investigated the effects of partial slip, viscous dissipation, heat generation or absorption and convective boundary condition on three dimensional magnetohydrodynamic flow of Casson fluid and heat and mass transfer past a permeable sheet which shrinks axisymmetrically in its own plate. The governing equations are transformed into a system of non linear ordinary differential equations by using the similarity transformations. The reduced systems of equations are solved by using the fourth order Runge-Kutta Gill procedure together with shooting technique. The results are presented graphically and in tabular form for various controlling parameters. The numerical results are validated by comparisons with previously published results in the literature.

II.   Mathematical Formulation

Consider a three-dimensional flow of an electrically conducting Cassonfluid due to a permeable axisymmetric shrinking sheet.The sheet is placed in the plane z=0 and the flow takes place in upper half plane z>0.The x and y axes are taken along the length and breadth of the sheet and z axis is perpendicular to the sheet,respectively (Figure A).A constant magnetic field with strength B_o is applied in the z-direction.The magnetic Reynolds number is taken tobe small,so that the induced magnetic field is neglected.The flow is caused by the sheet which shrinks axisymmetrically in its own plane.Suction is applied normal to sheet to contain the vorticity.The fluid adheres to the sheet partially and thus the motion of the fluid exhibits the slip condition.All the other fluid properties are assumed to be constant throughout the motion.
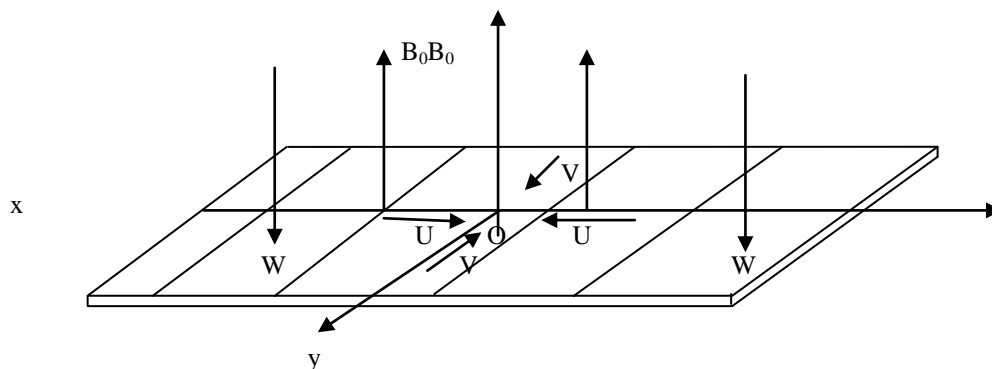
Figure A: Schematic diagram of the physical problem

The rheological equation of state for an isotropic flow of a Casson fluid (Eldabe and Salwa (1995)) can be expressed as

$$\tau_{ij} = \begin{cases} \left(\mu_B + \dfrac{p_y}{\sqrt{2\pi}}\right)2e_{ij}, & \pi>\pi_c \\[3mm] \left(\mu_B + \dfrac{p_y}{\sqrt{2\pi_c}}\right)2e_{ij}, & \pi<\pi_c \end{cases} \qquad (2.1)$$

where μ_B is plastic dynamic viscosity of the non-Newtonian fluid, p_y is the yield stress of fluid, π is the product of the component of deformation rate with itself, namely, $\pi = e_{ij}e_{ij}$, e_{ij} is the $(i, j)^{th}$ component of the deformation rate, and π_c is critical value of π based on non-Newtonian model.

With the usual Boussinesq and the boundary layer approximations, the governing equations of continuity, momentum, energy and species equations are written as follows;

Continuity equation
$$\frac{\partial u}{\partial x} + \frac{\partial v}{\partial y} + \frac{\partial w}{\partial z} = 0 \qquad (2.2)$$

Momentum equation
$$u\frac{\partial u}{\partial x} + v\frac{\partial u}{\partial y} + w\frac{\partial u}{\partial z} = -\frac{1}{\rho}\frac{\partial p}{\partial x} + \upsilon\left(1+\frac{1}{\beta}\right)\frac{\partial^2 u}{\partial z^2} - \frac{\sigma B_0^2}{\rho}u - \frac{\upsilon}{k'}u \qquad (2.3)$$

$$u\frac{\partial v}{\partial x} + v\frac{\partial v}{\partial y} + w\frac{\partial v}{\partial z} = -\frac{1}{\rho}\frac{\partial p}{\partial y} + \upsilon\left(1+\frac{1}{\beta}\right)\frac{\partial^2 u}{\partial z^2} - \frac{\sigma B_0^2}{\rho}v - \frac{\upsilon}{k'}v \qquad (2.4)$$

$$u\frac{\partial w}{\partial x} + v\frac{\partial w}{\partial y} + w\frac{\partial w}{\partial z} = -\frac{1}{\rho}\frac{\partial p}{\partial z} + \upsilon\left(1+\frac{1}{\beta}\right)\frac{\partial^2 u}{\partial z^2} \qquad (2.5)$$

$$u\frac{\partial T}{\partial x} + v\frac{\partial T}{\partial y} + w\frac{\partial T}{\partial z} = \frac{k}{\rho c_p}\left(\frac{\partial^2 T}{\partial x^2} + \frac{\partial^2 T}{\partial y^2} + \frac{\partial^2 T}{\partial z^2}\right) + \frac{Q_0}{\rho c_p}(T - T_\infty)$$
$$+ \frac{\mu}{\rho c_p}\left[2\left\{\left(\frac{\partial u}{\partial x}\right)^2 + \left(\frac{\partial v}{\partial y}\right)^2 + \left(\frac{\partial w}{\partial z}\right)^2\right\} + \left(\frac{\partial u}{\partial y} + \frac{\partial v}{\partial x}\right)^2 + \left(\frac{\partial u}{\partial z} + \frac{\partial w}{\partial x}\right)^2 + \left(\frac{\partial v}{\partial z} + \frac{\partial w}{\partial y}\right)^2\right] \quad (2.6)$$

$$u\frac{\partial C}{\partial x} + v\frac{\partial C}{\partial y} + w\frac{\partial C}{\partial z} = D_m\left(\frac{\partial^2 C}{\partial x^2} + \frac{\partial^2 C}{\partial y^2} + \frac{\partial^2 C}{\partial z^2}\right) - k_0\left(C - C_\infty\right) \qquad (2.7)$$

The boundary conditions for the velocity, temperature and concentration fields are
$$u = u_w + \lambda_0\frac{\partial u}{\partial z}, v = v_w + \lambda_0\frac{\partial v}{\partial z}, w = -W, -k\frac{\partial T}{\partial y} = h_f\left(T_f - T\right), C = C_w \text{ at } y = 0 \quad (2.8)$$

$$u \to 0, v \to 0, T \to T_\infty, C \to C_\infty \text{ as } y \to \infty \qquad (2.9)$$

Where (u, v, w) are the velocity component along the (x, y, z) directions respectively, $\beta = \mu_B\sqrt{2\pi_c}/P_y$ is the non-Newtonian Casson fluid parameter, p is the pressure, k′ is the permeability of the porous medium, W is the suction velocity from the surface, μ is the dynamic viscosity, $v = \frac{\mu}{\rho}$ is the kinematic viscosity, σ is the electrical conductivity, C_p is the specific heat at constant pressure, Q_0 is the volumetric rate of heat source or sink, D_m is the mass diffusivity, $u_w = -ax$ and $v_w = -ay$ are the shrinking velocities at the surface, a>0 is the Shrinking constant, T is the temperature of the fluid, T_f is the temperature at the surface, T_∞ is the free stream temperature, C is the concentration of the fluid, C_w is the concentration at the surface, C_∞ is the free stream concentration, ρ is the fluid density, k_0 is the chemical reaction rate constant, λ_0 is the initial value of the velocity slip factor.

Now, we introduce the following similarity transformations

$$u = axf'(\eta), v = ayf'(\eta), w = -2\sqrt{a\upsilon}f(\eta), \eta = \sqrt{\frac{a}{\upsilon}}z \qquad (2.10)$$

Where $\upsilon = \dfrac{\mu}{\rho}$ is the kinematic viscosity

$f(\eta)$ is the dimensionless stream function

The dimensionless temperature and concentration are

$$\theta(\eta) = \frac{T - T_\infty}{T_f - T_\infty} \qquad (2.11)$$

$$\phi(\eta) = \frac{C - C_\infty}{C_w - C_\infty} \qquad (2.12)$$

Equation (2.2) is identically satisfied by similarity transformations while equation (2.5) becomes

$$\frac{p}{\rho} = \upsilon\frac{\partial w}{\partial z} - \frac{w^2}{2} + Cons\tan t \qquad (2.13)$$

After the substitution of these transformations (2.10) – (2.12) along with the boundary conditions (2.8) and (2.9) in the equations (2.3), (2.4), (2.6) and (2.7), the resulting non-linear ordinary differential equations are written as follows:

$$\left(1 + \frac{1}{\beta}\right)f'''(\eta) + 2f(\eta)f''(\eta) - f'(\eta)^2 - \left(M + \frac{1}{K}\right)f'(\eta) = 0 \qquad (2.14)$$

$$\frac{1}{\Pr}\theta''(\eta) + 2f(\eta)\theta'(\eta) + Q\theta(\eta) + 12Ecf'(\eta)^2 + \left(Ec_x + Ec_y\right)f''(\eta)^2 = 0 \quad (2.15)$$

$$\frac{1}{Sc}\phi''(\eta) + 2f(\eta)\phi'(\eta) - Kr\phi(\eta) = 0 \qquad (2.16)$$

The corresponding boundary conditions are

$$f(0) = f_w, f'(0) = -1 + \lambda f''(0), \theta'(0) = -Bi(1 - \theta(0)), \phi(0) = 1$$

$$f' = \theta = \phi = 0 \text{ as } \eta \to \infty \qquad (2.17)$$

where the primes denote differentiation with respect to η

the dimensionless numbers in the above transformed equations are the Prandtl number (Pr), Eckert number (Ec), Ec_x and Ec_y are the local Eckert numbers along x and y directions respectively, and Schmidt number (Sc) which are defined as follows

$$\Pr = \frac{\mu c_p}{k}$$

$$Ec = \frac{\mu a}{\rho c_p(T_w - T_\infty)}$$

$$Ec_x = \frac{a^2 x^2}{c_p(T_w - T_\infty)}$$

$$Ec_y = \frac{a^2 y^2}{c_p(T_w - T_\infty)}$$

$$Sc = \frac{\upsilon}{D_m}$$

Moreover, $M = \dfrac{\sigma B_0^2}{a\rho}$ is the magnetic field parameter, $f_w = -\dfrac{W}{2\sqrt{a\upsilon}}$ is the suction (>0) parameter,

$\lambda = \lambda_0\sqrt{\dfrac{a}{\upsilon}}$ is the slip parameter, $K = \dfrac{ak'}{\upsilon}$ is the permeability parameter, $Bi = \dfrac{h_f}{k}\sqrt{\dfrac{\upsilon}{a}}$ is the convective

parameter, $Q = \dfrac{Q_0}{a\rho c_p}$ is the heat generation (>0) or absorption (<0) parameter and $Kr = \dfrac{k_0}{a}$ is the chemical

reaction parameter.

The parameters of significant interest for the present problem are the skin-friction coefficient C_f, on

the surface along x and y directions, which are denoted by C_{fx} and C_{fy}, respectively, local Nusselt

number Nu_x and local Sherwood number Sh_x which are given by

$$C_{fx} = \frac{\tau_{wx}}{\rho u_w^2/2}$$

$$C_{fy} = \frac{\tau_{wy}}{\rho v_w^2/2}$$

$$Nu_x = \frac{xq_w}{k(T_w - T_\infty)}$$ (2.18)

$$Sh_x = \frac{xq_m}{D_m(C_w - C_\infty)}$$

Where τ_{wx} and τ_{wy} are the local wall shear stresses along the x and y respectively, the heat transfer

from the surface q_w and the mass transfer from the surface q_m are defined by

$$\tau_{wx} = \mu\left(1 + \frac{1}{\beta}\right)\left(\frac{\partial u}{\partial z}\right)_{z=0}$$

$$\tau_{wy} = \mu\left(1 + \frac{1}{\beta}\right)\left(\frac{\partial u}{\partial z}\right)_{z=0}$$

$$q_w = -k\left(\frac{\partial T}{\partial y}\right)_{y=0}$$ (2.19)

$$q_m = -D_m\left(\frac{\partial C}{\partial y}\right)_{y=0}$$

Using the similarity variables (2.10) – (2.12), the resulting equations are

$$2C_{fx}\,\text{Re}_x^{1/2} = \left(1 + \frac{1}{\beta}\right)f''(0)$$

$$2C_{fy}\,\text{Re}_y^{1/2} = \left(1 + \frac{1}{\beta}\right)f''(0)$$ (2.20)

$$Nu_x\,\text{Re}_x^{-1/2} = -\theta'(0)$$

$$Sh_x\,\text{Re}_x^{-1/2} = -\phi'(0)$$

Where $\text{Re}_x = \dfrac{u_w x}{\upsilon}$ and $\text{Re}_y = \dfrac{v_w y}{\upsilon}$ are the local Reynolds numbers along x and y directions respectively.

III.   Solution Of The Problem

The set of equations (2.12) to (2.15)were reduced to a system of first-order differential equations and solved using a MATLAB boundary value problem solver called **bvp4c**. This program solves boundary value problems for ordinary differential equations of the form $y' = f(x, y, p), a \leq x \leq b$, by implementing a collocation method subject to general nonlinear, two-point boundary conditions $g(y(a), y(b), p)$. Here *p*is a vector of unknown parameters. Boundary value problems (BVPs) arise in most diverse forms. Just about any BVP can be formulated for solution with **bvp4c**. The first step is to write the *ODEs* as a system of first order ordinary differential equations. The details of the solution method are presented in Shampine and Kierzenka (2000).

IV.   Results And Discussion

The governing equations (2.14) - (2.16) subject to the boundary conditions (2.17) are integrated as described in section 3. In order to get a clear insight of the physical problem, the velocity, angular velocity, temperature and concentration have been discussed by assigning numerical values to the parameters encountered in the problem.

In order to verify the accuracy of our present results, comparisons have been made with the available results ofSrinivasacharya and Upendar (2013) in the literature which are shown in table 1 relating to skin-friction coefficient($f''(0)$) and local Nusselt number ($\theta'(0)$) with M = Sc = Ec = Ec$_x$= Ec$_y$ = Q = λ = 0 and $\beta \to \infty, K \to \infty$.It is eatablished that the results obtained in the present work shows a good agreement with the previously published results.

Figures 1(a)-1(c) depicts the effect of magnetic parameter (M) in dimensionless velocity, temperature and concentration distributions respectively. The effect of magnetic parameter is explicated by setting the values of the other parameters to be constant for β = 2, K = 0.5, Pr = 2, Q = 0.5, Ec = 0.1, Ec$_x$ = 0.1, Ec$_y$ = 0.1, Sc = 1, λ = 0.3, Kr = 0.3, f$_w$ = 1 & Bi = 0.1.It is seen that the dimensionless velocity distribution of the fluid decreases with an increasing the magnetic parameter (see figure1a). The magnetic parameter is found to increase the velocity at all points of the flow field. That is momentum boundary layer thickness decreases throughout the boundary layer region. It is because that the application of transverse magnetic field will result in a resistive type force (Lorentz force) similar to drag force which tends to resist the fluid flow and thus reducing its velocity. The dimensionless temperature and concentration distribution of the fluid decreases throughout the boundary layer with raising the magnetic parameter (figure 1(b)&1(c)). These results were similar to that of Jat and Rojatia (2014).

Figures 2(a)-2(c) shows that the effect of Cassonparameter (β) on dimensionless velocity, temperature and concentration distributions respectively. The other parameters are set constantly atM = 0.5, K = 0.5, Pr = 2, Q = 0.5, Ec = 0.1, Ec$_x$ = 0.1, Ec$_y$ = 0.1, Sc = 1, λ = 0.3, Kr = 0.3, f$_w$ = 1 & Bi = 0.1. It is observed that dimensionless velocitydistribution of the fluid increases with an increasing the values of non-Newtonian Cassonparameter (Figures 2(a)).Thedimensionless temperature and concentration distribution of the fluid decreases with the influence of non-Newtonian Cassonparameter (Figure 2(b)& 2(c)).

Figures 3(a)-3(c) depicts that the effect of permeability parameter (*K*) on dimensionless velocity, temperature and concentration distributions respectively. The other parameters are set constantly at M = 0.5, β = 2, Pr = 2, Q = 0.5, Ec = 0.1, Ec$_x$ = 0.1, Ec$_y$ = 0.1, Sc = 1, λ = 0.3, Kr = 0.3, f$_w$ = 1 & Bi = 0.1. It is observed that dimensionless velocity distribution of the fluid decreases with an increasing the values of permeability parameter (Figures 3(a)). The dimensionless temperature and concentration distribution of the fluid increases with the influence of permeability parameter (Figure 3(b)& 3(c)).

Figures 4(a)-4(c) depicts that the effect of velocity slip parameter (λ) on dimensionless velocity, temperature and concentration distributions respectively. The other parameters are set constantly at M = 0.5, β = 2, K = 0.5, Pr = 2, Q = 0.5, Ec = 0.1, Ec$_x$ = 0.1, Ec$_y$ = 0.1, Sc = 1, Kr = 0.3, f$_w$ = 1 & Bi = 0.1. It is observed that dimensionless velocity distribution of the fluid increases with an increasing the values of velocity slip parameter (Figures 4(a)). The dimensionless temperature and concentration distribution of the fluid decreases with the influence of velocity slip parameter (Figure 4(b)& 4(c)).

Figures 5(a)-5(c) depicts that the effect of suction parameter (f$_w$) on dimensionless velocity, temperature and concentration distributions respectively. The other parameters are set constantly at M = 0.5, β = 2, K = 0.5, Pr = 2, Q = 0.5, Ec = 0.1, Ec$_x$ = 0.1, Ec$_y$ = 0.1, Sc = 1, λ = 0.3, Kr = 0.3 & Bi = 0.1. It is observed that dimensionless velocity distribution of the fluid increases with an increasing the values of suction parameter (Figures 5(a)). The dimensionless temperature and concentration distribution of the fluid decreases with the influence of suction parameter (Figure 5(b) & 5(c)).

For the constant parametersM = 0.5, β = 2, K = 0.5, Pr = 2, Ec = 0.1, Ec$_x$ = 0.1, Ec$_y$ = 0.1, Sc = 1, λ = 0.3, Kr = 0.3, f$_w$ = 1 & Bi = 0.1. The effect of heat source (Q > 0) or sink parameter (Q < 0) on the temperature is plotted in Figure 6. It can be showed that the effect of heat absorption results in a fall of temperature since

heat resulting from the wall is absorbed. Obviously, the heat generation leads to an increase in temperature throughout the entire boundary layer. Furthermore, it should be noted that for the case of heat generation, the fluid temperature become maximum in the fluid layer adjacent to the wall rather at the wall. In fact, the heat generation effect not only has the tendency to increase the fluid temperature but also increase the thermal boundary layer thickness. Due to heat absorption, it is observed that the fluid temperature as well as the thermal boundary layer thickness is decreased. No significance in heat distribution is observed among the fluids in the presence of heat absorption.

Figures 7 depicts that the effect of convective parameter (Bi) on dimensionless temperature distribution respectively. The other parameters are set constantly at $M = 0.5$, $\beta = 2$, $K = 0.5$, $Pr = 2$, $Q = 0.5$, $Ec = 0.1$, $Ec_x = 0.1$, $Ec_y = 0.1$, $Sc = 1$, $\lambda = 0.3$, $Kr = 0.3$, $f_w = 1$. It is observed that dimensionless temperature distribution of the fluid increases with an increasing the values of convective parameter(Figures 7).

Setting the other parameters to be constants as $M = 0.5$, $\beta = 2$, $K = 0.5$, $Q = 0.5$, $Ec = 0.1$, $Ec_x = 0.1$, $Ec_y = 0.1$, $Sc = 1$, $\lambda = 0.3$, $Kr = 0.3$, $f_w = 1$ & $Bi = 0.1$. Figure 8 shows that the effect of Prandtl number (Pr) on dimensionless temperature. It can be observed that the dimensionless temperature is decreased on increasing Prandtl number. Physically, increasing Prandtl number becomes a key factor to reduce the thickness of the thermal boundary layer

The effect of Eckert number (Ec) on the dimensionless temperature profiles is plotted in Figures 9. Setting the other parameters to be constants as $M = 0.5$, $\beta = 2$, $K = 0.5$, $Pr = 2$, $Q = 0.5$, $Ec_x = 0.1$, $Ec_y = 0.1$, $Sc = 1$, $\lambda = 0.3$, $Kr = 0.3$, $f_w = 1$ & $Bi = 0.1$. These figures reveal that the temperature profiles increase with increasing values of Eckert number. Owing to viscous heating, the increase in the fluid temperature is enhanced and appreciable for higher value of Eckert number. In other words, increasing the Eckert number leads to a coolness of the wall. Consequently, a transfer of heat to the fluid occurs, which causes a rise in the temperature of the fluid.

Figures 10(a) & 10(b) depicts that the effect of local Eckert numbers Ec_x and Ec_y on dimensionless temperature distribution respectively. The other parameters are set constantly at $M = 0.5$, $\beta = 2$, $K = 0.5$, $Pr = 2$, $Q = 0.5$, $Ec = 0.1$, $Sc = 1$, $\lambda = 0.3$, $Kr = 0.3$, $f_w = 1$ & $Bi = 0.1$. It is observedfrom figure 10(a) that with increasing values of Ec_x the temperature of the fluid increases fastly near the surface more than for from the sheet and this also happens because of the energy is stored in the fluid due to the fractional heating. The same phenomenon occurs for Ec_y in figure 10(b).

Setting the other parameters to be constants as $M = 0.5$, $\beta = 2$, $K = 0.5$, $Pr = 2$, $Q = 0.5$, $Ec = 0.1$, $Ec_x = 0.1$, $Ec_y = 0.1$, $\lambda = 0.3$, $Kr = 0.3$, $f_w = 1$ & $Bi = 0.1$. Figure 12 shows that the effect of Schmidt number (Sc) on dimensionless concentration distribution. It can be observed that the dimensionless concentration distribution is decreased on increasing Schmidt number.

Setting the other parameters to be constants as $M = 0.5$, $\beta = 2$, $K = 0.5$, $Pr = 2$, $Q = 0.5$, $Ec = 0.1$, $Ec_x = 0.1$, $Ec_y = 0.1$, $Sc = 1$, $\lambda = 0.3$, $f_w = 1$ & $Bi = 0.1$. Figure 13 shows that the effect of chemical reaction parameter (Kr) on dimensionless concentration distribution. It can be observed that the dimensionless concentration distribution is decreased on increasing chemical reaction parameter.

The effects of the magnetic parameter(M),Casson fluid parameter(β),permeabilityparameter (K),slip parameter(λ),suction parameter(f_w) on the local skin friction coefficient is illustrated in Table 2. From this table it is observe that local skin friction coefficient increase when magnetic field and suction are imposed.On the other hand the local skin friction coefficient decreased with increasing Casson fluid parameter, permeability parameter and slip parameter.

Table 3 shows the values of local nusselt number obtained for the variation of the magnetic parameter(M),Casson fluid parameter(β), permeability parameter (K),Prandtl number(Pr), heat generation or absorption parameter(Q),Eckert number(Ec),local Eckert numbers along x-axis and y-axis be Ec_x and Ec_y,Schimdt number(Sc),Slip parameter(λ),suction parameter(f_w) and convective parameter (Bi).For the table the heat transfer rate shows a rapid rise for imposed permeability parameter (K),Prandtl number(Pr),Eckert number(Ec),local Eckert numbers Ec_x and Ec_y,slip parameter,suction parameter and convectiveparameter. Further on increasing magnetic parameter,Casson fluid parameter, heat generation or absorption parameter and Schimdt number, it is noted that the heat transfer decreases rapidly.

Table 4 display the values of the local Sherwood number for the variations of the parameters magnetic parameter(M),Casson fluid parameter(β),permeability parameter (K),Schmidt number(Sc),chemical reaction parameter (Kr), slip parameter(λ),suction parameter(f_w).It can be understood from the table that the local Sherwood number decreases for the increasing of the permeability parameter.In other words the mass transfer rate increases on increasing the magnetic parameter,Casson fluid parameter,Schmidt number,chemical reaction parameter, slip parameter, suction parameter.

V. Conclusions

This paper investigated the effects of partial slip, viscous dissipation, heat generation or absorption and convective boundary condition on three dimensional magnetohydrodynamic flow of Casson fluid and heat and mass transfer past a permeable sheet which shrinks axisymmetrically in its own plate. The governing equations are approximated to a system of non-linear ordinary differential equations by similarity transformation. Numerical calculations are carried out for various values of the dimensionless parameters of the problem. It has been found that

1. The increase in the values of the magnetic parameter leads to a significant increase in flow velocity and a significant decrease in flow temperature and concentration profiles in the presence of slip parameter.
2. On increasing the values of Cassonfluid parameter, an increase is observed in flow velocity whereas the flow temperature and concentration is decreased in the presence of slip parameter.
3. When the permeability parameter increases, the resultant flow velocity decreased. Thickness thermal and concentration boundary layers significantly increase away from the surface when the permeability parameter increases in the presence of slip parameter.
4. When the slip parameter increases, the momentum boundary layer thickness considerably increase whereas temperature and concentration boundary layer thickness is decreased and same results were found in the effect of suction parameter.
5. The temperature distribution across the surface in the presence of heat generation is more significantly higher than in the absence of the heat generation.
6. Thermal boundary layer thickness significantly increases by an increasing the convective parameter.
7. On increasing the Schmidt number and chemical reaction parameter, the concentration boundary layer thickness significantly decreased.
8. When the slip parameter is imposed, the local skin-friction coefficient is decreased whereas the heat and mass transfer rates increased.

Table 1 Comparison of $f''(0)$ and $\theta'(0)$ with the available results in literature for M $=$Sc $=$ Ec $=$ Ec$_x=$ Ec$_y =$ Q $= \lambda = 0$ and $\beta \to \infty, K \to \infty.$

$f''(0)$		$\theta'(0)$	
Present study	Srinivasacharya and Upendar (2013)	Present study	Srinivasacharya and Upendar (2013)
0.739502	0.7395	- 0.595092	- 0.5950
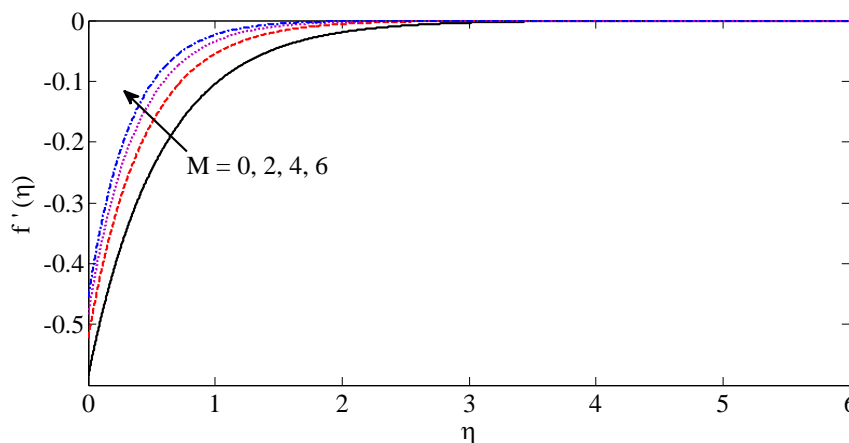
Figure 1(a)Dimensionless velocitydistribution for different values of*M* with β = 2, K = 0.5, Pr = 2, Q = 0.5, Ec = 0.1, Ec$_x$ = 0.1, Ec$_y$ = 0.1, Sc = 1, λ = 0.3, Kr = 0.3, f$_w$ = 1 & Bi = 0.1.
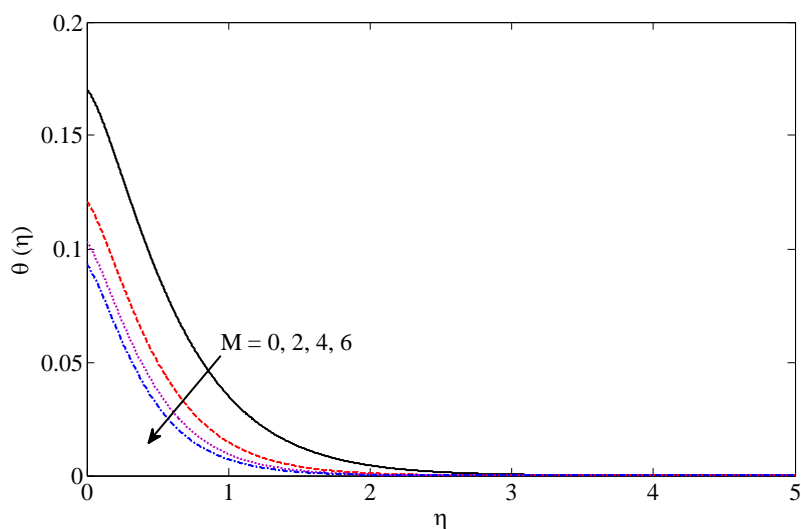
Figure 1(b)Dimensionless temperature distribution for different values of *M*with β = 2, K = 0.5, Pr = 2, Q = 0.5, Ec = 0.1, Ec$_x$ = 0.1, Ec$_y$ = 0.1, Sc = 1, λ = 0.3, Kr = 0.3, f$_w$ = 1 & Bi = 0.1.
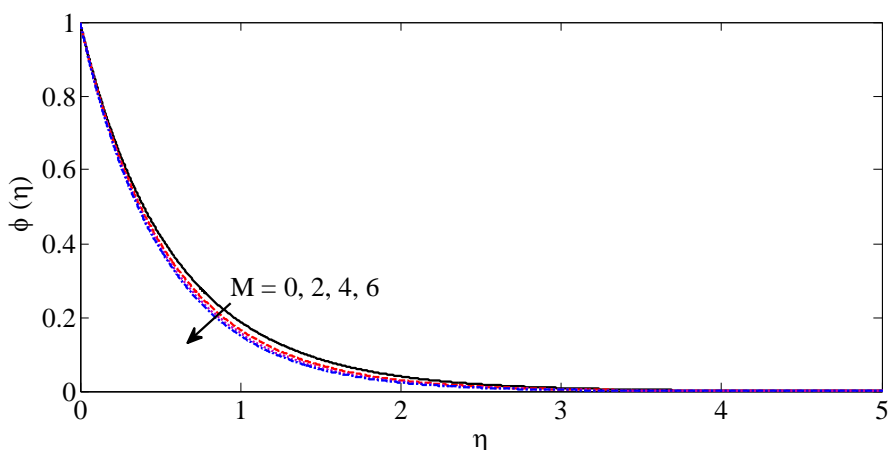
Figure 1(c)Dimensionless concentration distribution for different values of *M* with β = 2, K = 0.5, Pr = 2, Q = 0.5, Ec = 0.1, Ec$_x$ = 0.1, Ec$_y$ = 0.1, Sc = 1, Kr = 0.3, λ = 0.3, f$_w$ = 1 & Bi = 0.1.
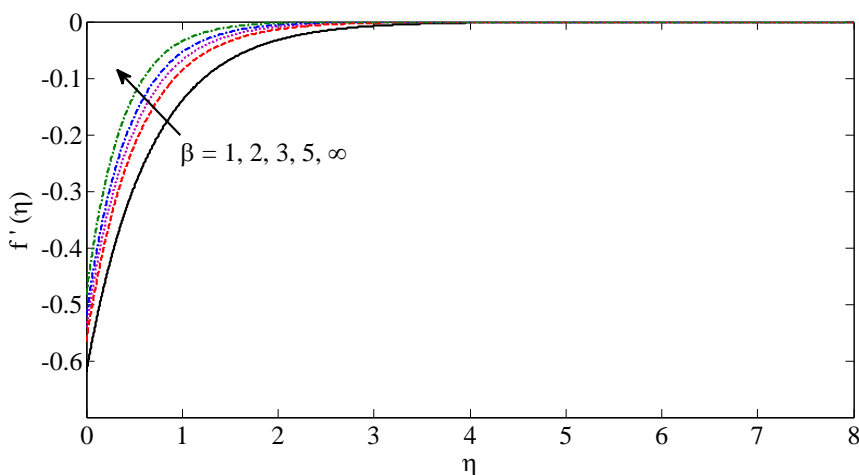
Figure 2(a)Dimensionless velocity distribution for different values of*β* with M = 0.5,K = 0.5, Pr = 2, Q = 0.5, Ec = 0.1, Ec$_x$ = 0.1, Ec$_y$ = 0.1, Sc = 1, Kr = 0.3, λ = 0.3, f$_w$ = 1 & Bi = 0.1.
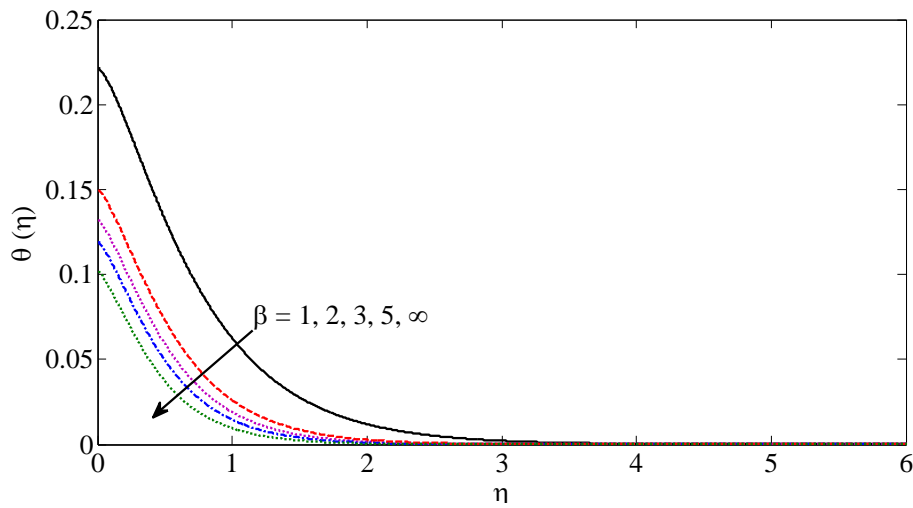
Figure 2(b)Dimensionless temperature distribution for different values of*β* with M = 0.5, K = 0.5, Pr = 2, Q = 0.5, Ec = 0.1, Ec$_x$ = 0.1, Ec$_y$ = 0.1, Kr = 0.3, Sc = 1, λ = 0.3, f$_w$ = 1 & Bi = 0.1.
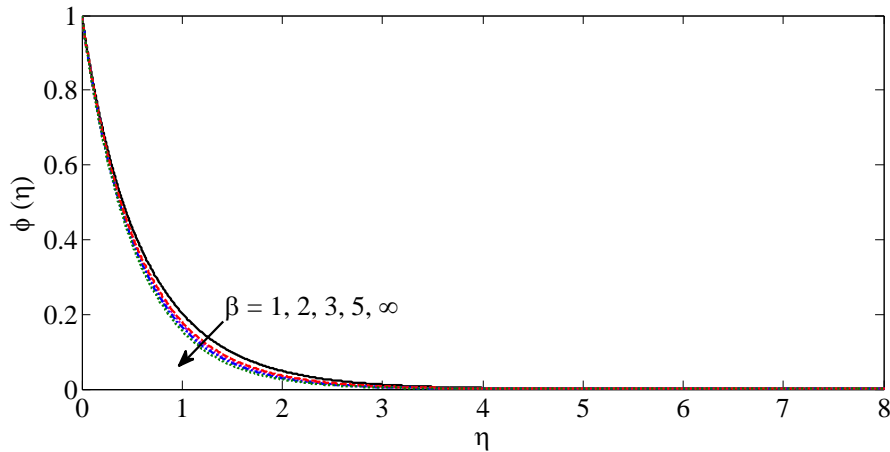
Figure 2(c)Dimensionless concentration distribution for different values of *β* with M = 0.5, K = 0.5, Pr = 2, Q = 0.5, Ec = 0.1, Ec$_x$ = 0.1, Ec$_y$ = 0.1, Kr = 0.3, Sc = 1, λ = 0.3, f$_w$ = 1 & Bi = 0.1.
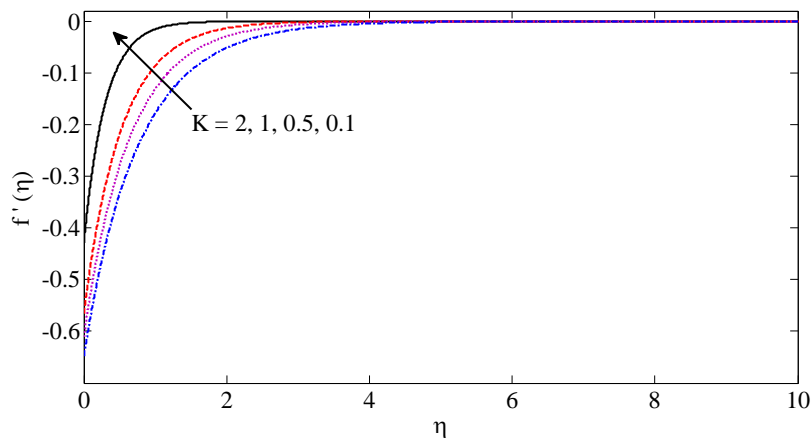
Figure 3(a)Dimensionless velocity distribution for different values of *K* with M = 0.5, β = 2, Pr = 2, Q = 0.5, Ec = 0.1, Ec$_x$ = 0.1, Ec$_y$ = 0.1, Sc = 1, Kr = 0.3, λ = 0.3, f$_w$ = 1 & Bi = 0.1.
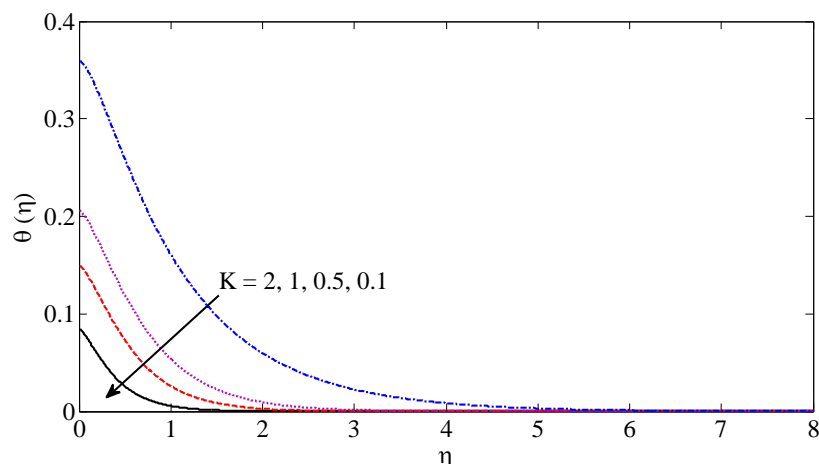
Figure 3(b)Dimensionless temperature distribution for different values of$K$ with M = 0.5, β = 2, Pr = 2, Q = 0.5, Ec = 0.1, Ec_x = 0.1, Ec_y = 0.1, Kr = 0.3, Sc = 1, λ = 0.3, f_w = 1 & Bi = 0.1.
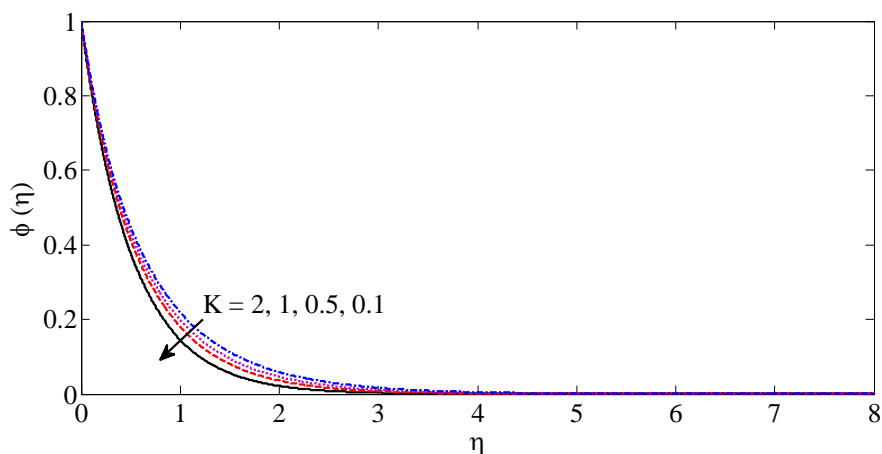
Figure 3(c)Dimensionless concentration distribution for different values of K with M = 0.5, β = 2, Pr = 2, Q = 0.5, Ec = 0.1, Ec_x = 0.1, Ec_y = 0.1, Kr = 0.3, Sc = 1, λ = 0.3, f_w = 1 & Bi = 0.1.
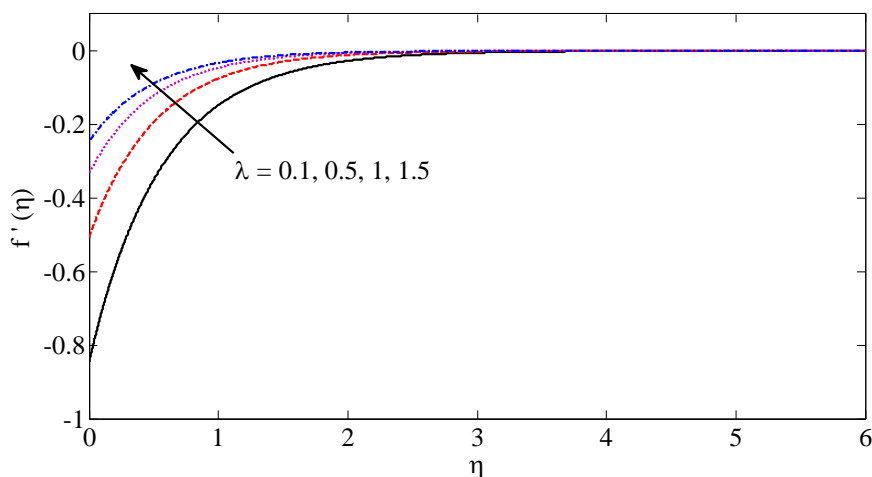
Figure 4(a)Dimensionless velocity distribution for different values of$λ$ with M = 0.5, β = 2, K = 0.5, Pr = 2, Q = 0.5, Ec = 0.1, Ec_x = 0.1, Ec_y = 0.1, Kr = 0.3, Sc = 1, f_w = 1 & Bi = 0.1.
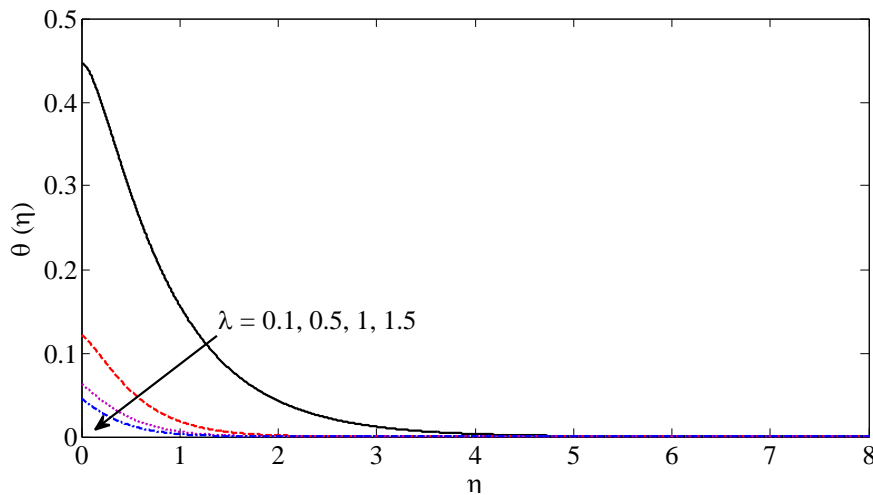
Figure 4(b)Dimensionless temperature distribution for different values of λ with M = 0.5, β = 2, K = 0.5, Pr = 2, Q = 0.5, Ec = 0.1, Ec_x = 0.1, Ec_y = 0.1, Kr = 0.3, Sc = 1, f_w = 1 & Bi = 0.1.
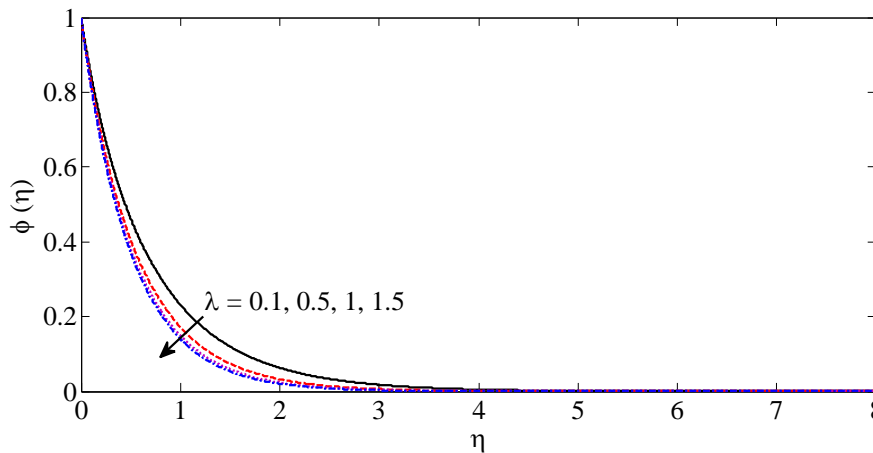
Figure 4(c)Dimensionless concentration distribution for different values of λ with M = 0.5, β = 2, K = 0.5, Pr = 2, Q = 0.5, Ec = 0.1, Ec_x = 0.1, Ec_y = 0.1, Sc = 1, Kr = 0.3, f_w = 1 & Bi = 0.1.
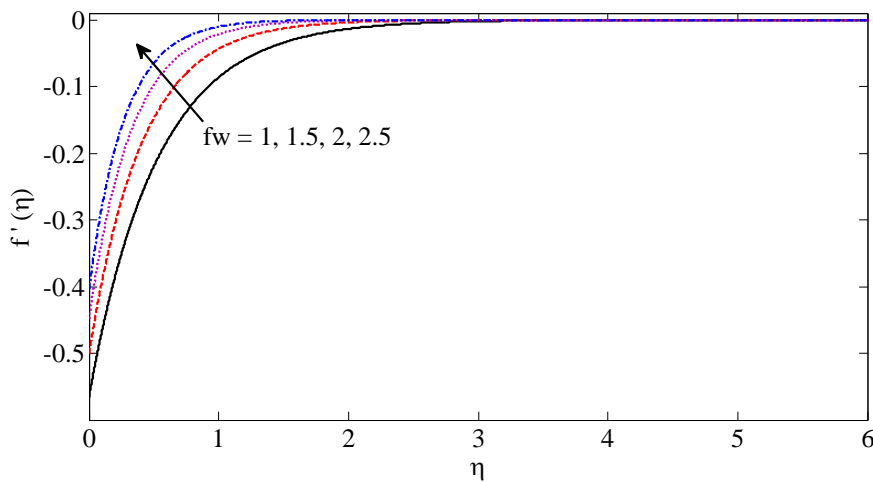
Figure 5(a)Dimensionless velocity distributionfor different values of f_w with M = 0.5, β = 2, K = 0.5, Pr = 2, Q = 0.5, Ec = 0.1, Ec_x = 0.1, Ec_y = 0.1, Sc = 1, Kr = 0.3, λ = 0.3, & Bi = 0.1.
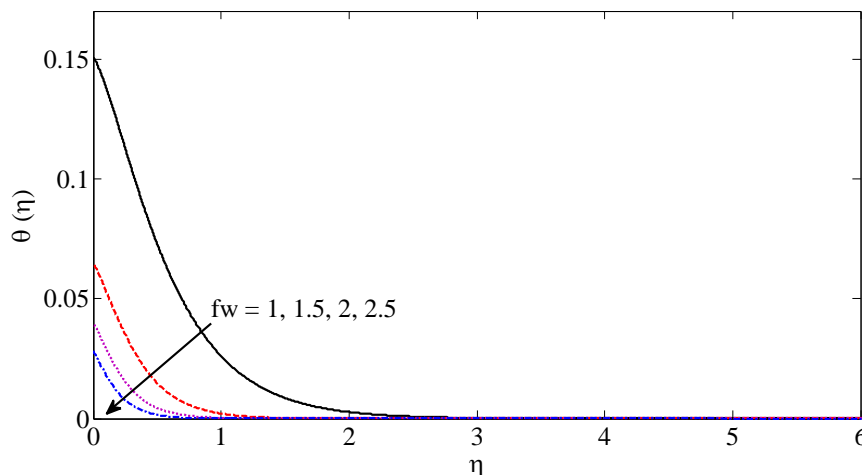
Figure 5(b)Dimensionless temperature distribution for different values of f_w with M = 0.5, β = 2, K = 0.5, Pr = 2, Q = 0.5, Ec = 0.1, Ec_x = 0.1, Ec_y = 0.1, Sc = 1, Kr = 0.3, λ = 0.3, & Bi = 0.1.
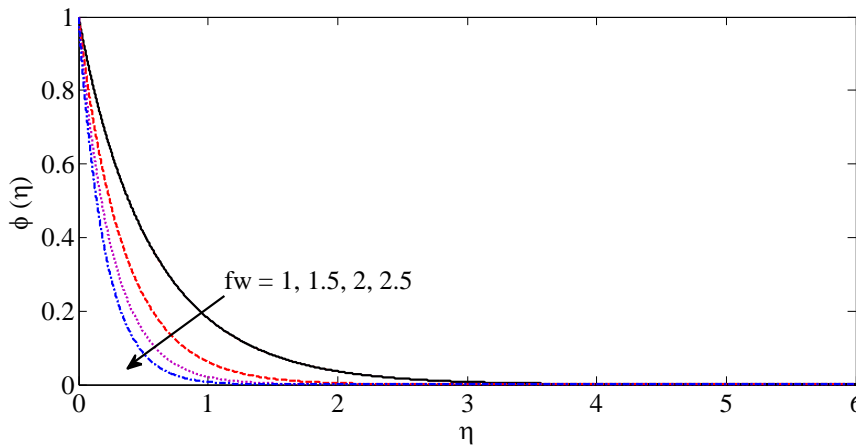
Figure 5(c)Dimensionless concentration distribution for different values of f_w with M = 0.5, β = 2, K = 0.5, Pr = 2, Q = 0.5, Ec = 0.1, Ec_x = 0.1, Ec_y = 0.1, Kr = 0.3, Sc = 1, λ = 0.3 & Bi = 0.1.
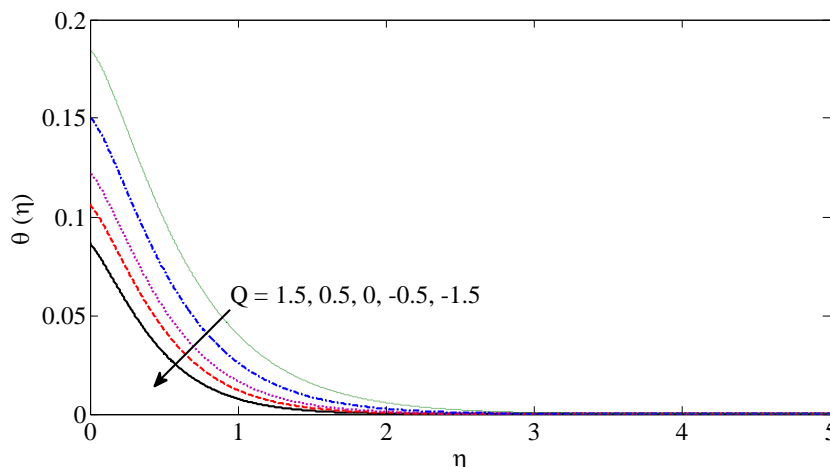
Figure 6 Dimensionless temperature distribution for different values of Q with M = 0.5, β = 2, K = 0.5, Pr = 2, Ec = 0.1, Ec_x = 0.1, Ec_y = 0.1, Sc = 1, λ = 0.3, Kr = 0.3,f_w = 1 & Bi = 0.1.
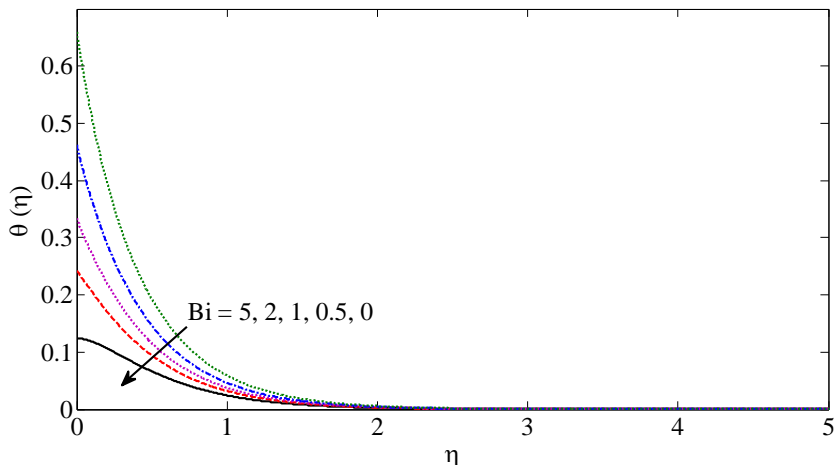
Figure 7Dimensionless temperature distribution for different values of *Bi* withM = 0.5, β = 2, K = 0.5, Pr = 2, Q = 0.5, Ec = 0.1, Ec$_x$ = 0.1, Ec$_y$ = 0.1, Kr = 0.3, Sc = 1, λ = 0.3, f$_w$ = 1.
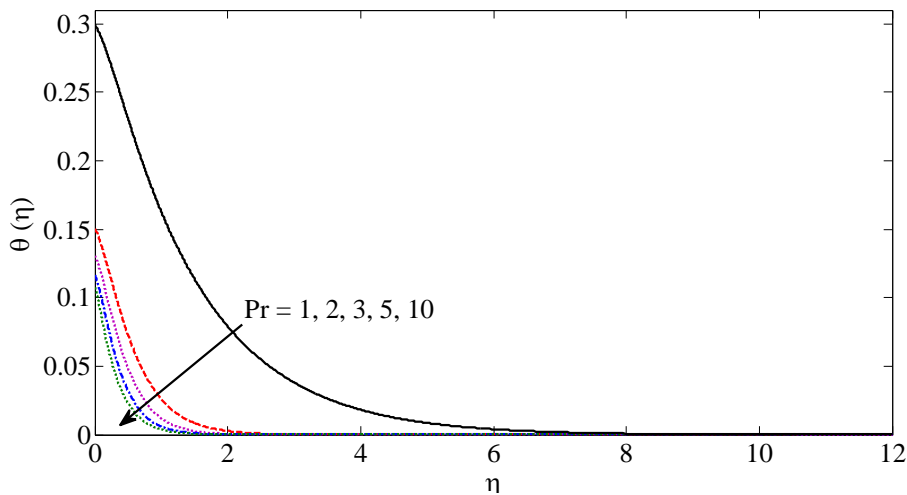
Figure 8Dimensionless temperature distribution for different values of *Pr* with M = 0.5, β = 2, K = 0.5, Q = 0.5, Ec = 0.1, Ec$_x$ = 0.1, Ec$_y$ = 0.1, Kr = 0.3, Sc = 1, λ = 0.3, f$_w$ = 1 & Bi = 0.1.
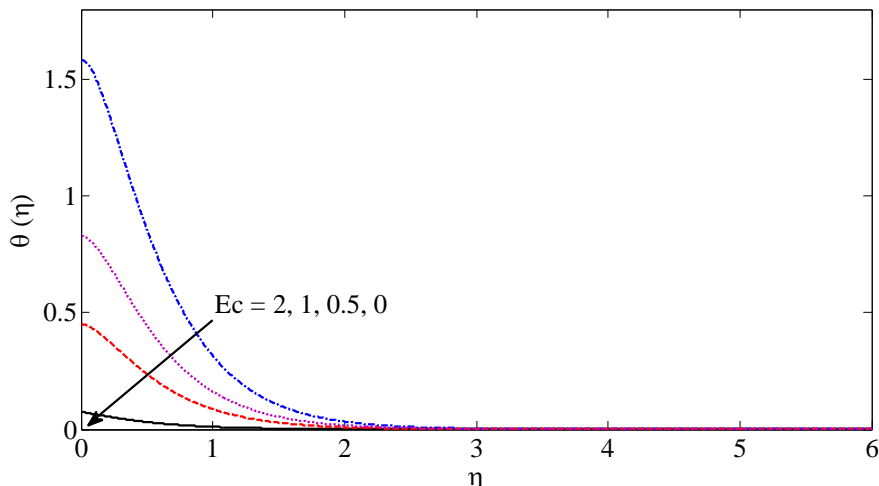
Figure 9Dimensionless temperature distribution for different values of *Ec* withM = 0.5, β = 2, K = 0.5, Pr = 2, Q = 0.5, Ec$_x$ = 0.1, Ec$_y$ = 0.1, Kr = 0.3, Sc = 1, λ = 0.3, f$_w$ = 1 & Bi = 0.1.
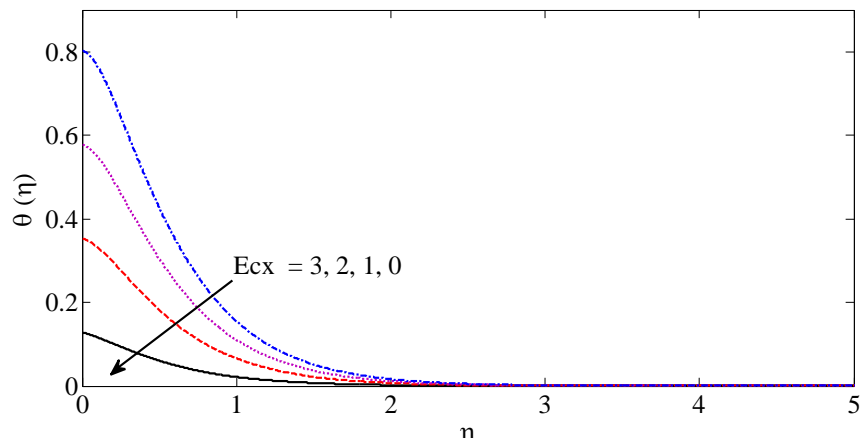
Figure 10(a)Dimensionless temperature distribution for different values of Ec_x withM = 0.5, β = 2, K = 0.5, Pr = 2, Q = 0.5, Ec = 0.1, Ec_y = 0.1, Kr = 0.3, Sc = 1, λ = 0.3, f_w = 1 & Bi = 0.1.
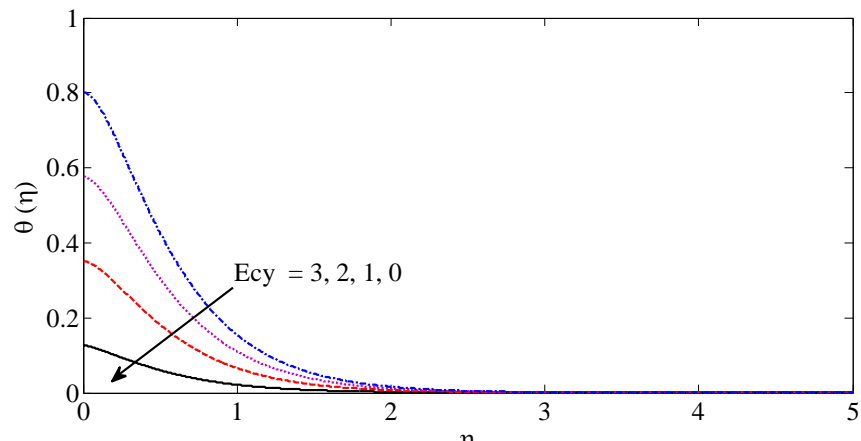
Figure 10(b)Dimensionless temperature distribution for different values of $Ec_y$with M = 0.5, β = 2, K = 0.5, Pr = 2, Q = 0.5, Ec = 0.1, Ec_x = 0.1, Kr = 0.3, Sc = 1, λ = 0.3, f_w = 1 & Bi = 0.1.
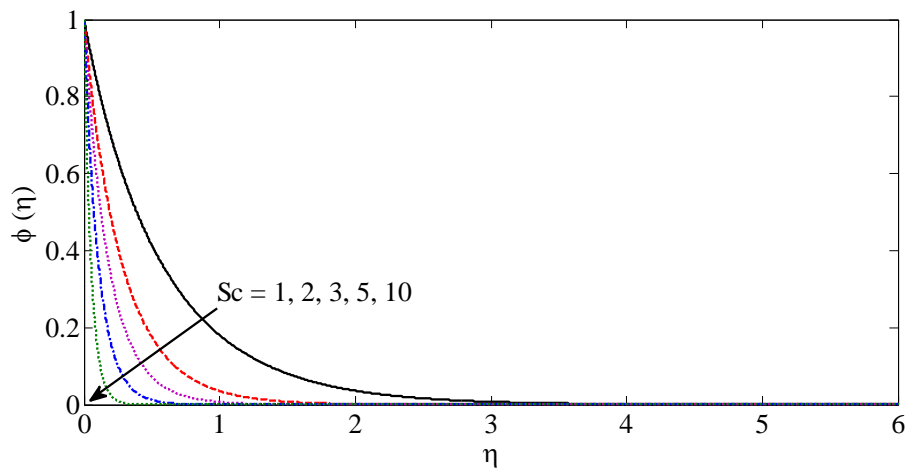
Figure 11Dimensionless concentration distribution for different values of Sc for M = 0.5, β = 2, K = 0.5, Pr = 2, Q = 0.5, Ec = 0.1, Ec_x = 0.1, Kr = 0.3,Ec_y = 0.1, λ = 0.3, f_w = 1 & Bi = 0.1.
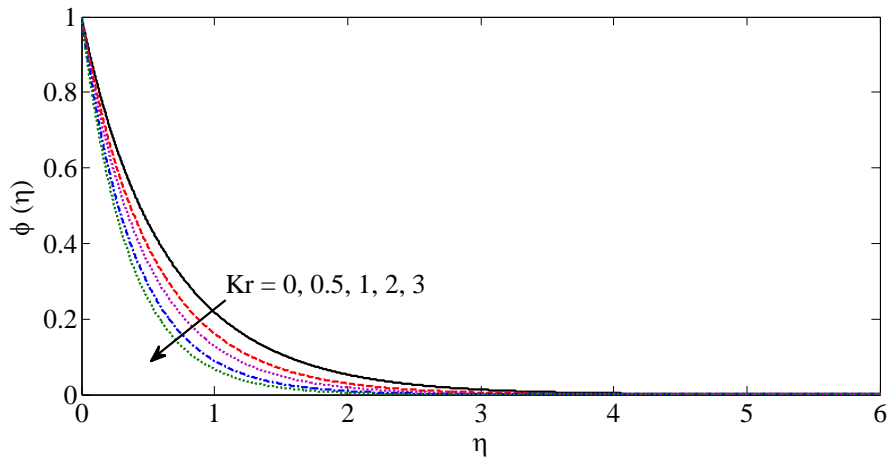
Figure 12 Dimensionless concentration distribution for different values ofKr for M = 0.5, β = 2, K = 0.5, Pr = 2, Q = 0.5, Ec = 0.1, Ec$_x$ = 0.1, Ec$_y$ = 0.1, Sc = 1, λ = 0.3, f$_w$ = 1 & Bi = 0.1.

Table 2 Numerical results for skin friction coefficient $-f''(0)$ for M, β, K, λ and f$_w$ withPr = 2, Q = 0.5, Ec = 0.1, Ec$_x$ = 0.1, Ec$_y$ = 0.1, Kr = 0.3, Sc = 1 & Bi = 0.1.

M	β	K	λ	f$_w$	$-f''(0)$
0.5	0.5	0.5	0.4	1	2.323678
1	0.5	0.5	0.4	1	2.469651
1.5	0.5	0.5	0.4	1	2.592234
2	0.5	0.5	0.4	1	2.698407
0.5	1	0.5	0.4	1	1.898467
0.5	1.5	0.5	0.4	1	1.725149
0.5	2	0.5	0.4	1	1.629634
0.5	0.5	1	0.4	1	1.887536
0.5	0.5	1.5	0.4	1	1.620660
0.5	0.5	2	0.4	1	1.384891
0.5	0.5	0.5	0	1	3.075574
0.5	0.5	0.5	0.5	1	2.175515
0.5	0.5	0.5	0.75	1	1.867220
0.5	0.5	0.5	1	1	1.629111
0.5	0.5	0.5	0.4	1.5	2.669124
0.5	0.5	0.5	0.4	2	2.993411
0.5	0.5	0.5	0.4	2.5	3.289713
0.5	0.5	0.5	0.4	3	3.557055

Table 3 Numerical results for local Nusselt number $-\theta'(0)$ for M, β, K, Pr, Q, Ec, Ec$_x$, Ec$_y$, Sc, λ, f$_w$ and Bi with Kr = 0.3.

M	β	K	Pr	Q	Ec	Ec$_x$	Ec$_y$	Sc	λ	f$_w$	Bi	$-\theta'(0)$
0.5	0.5	0.5	1	0.5	0.1	0.1	0.1	1	0.4	1	0.1	0.193061
1	0.5	0.5	1	0.5	0.1	0.1	0.1	1	0.4	1	0.1	0.032361
1.5	0.5	0.5	1	0.5	0.1	0.1	0.1	1	0.4	1	0.1	0.065662
2	0.5	0.5	1	0.5	0.1	0.1	0.1	1	0.4	1	0.1	0.080852
0.5	1	0.5	1	0.5	0.1	0.1	0.1	1	0.4	1	0.1	0.228008
0.5	1.5	0.5	1	0.5	0.1	0.1	0.1	1	0.4	1	0.1	0.078071
0.5	2	0.5	1	0.5	0.1	0.1	0.1	1	0.4	1	0.1	0.070067
0.5	0.5	1	1	0.5	0.1	0.1	0.1	1	0.4	1	0.1	0.058972
0.5	0.5	1.5	1	0.5	0.1	0.1	0.1	1	0.4	1	0.1	0.075441
0.5	0.5	2	1	0.5	0.1	0.1	0.1	1	0.4	1	0.1	0.251679
0.5	0.5	0.5	2	0.5	0.1	0.1	0.1	1	0.4	2	0.1	0.093197
0.5	0.5	0.5	3	0.5	0.1	0.1	0.1	1	0.4	2	0.1	0.093697
0.5	0.5	0.5	5	0.5	0.1	0.1	0.1	1	0.4	2	0.1	0.094091
0.5	0.5	0.5	1	-1.5	0.1	0.1	0.1	1	0.4	1	0.1	0.085092
0.5	0.5	0.5	1	-0.5	0.1	0.1	0.1	1	0.4	1	0.1	0.078487
0.5	0.5	0.5	1	0	0.1	0.1	0.1	1	0.4	1	0.1	0.067104
0.5	0.5	0.5	1	1.0	0.1	0.1	0.1	1	0.4	1	0.1	0.066669
0.5	0.5	0.5	1	1.5	0.1	0.1	0.1	1	0.4	1	0.1	0.040959

0.5	0.5	0.5	1	0.5	0	0.1	0.1	1	0.4	1	0.1	0.121981
0.5	0.5	0.5	1	0.5	0.5	0.1	0.1	1	0.4	1	0.1	0.475308
0.5	0.5	0.5	1	0.5	1	0.1	0.1	1	0.4	1	0.1	0.828815
0.5	0.5	0.5	1	0.5	2	0.1	0.1	1	0.4	1	0.1	1.535828
0.5	0.5	0.5	1	0.5	0.1	0	0.1	1	0.4	1	0.1	1.528955
0.5	0.5	0.5	1	0.5	0.1	0.5	0.1	1	0.4	1	0.1	1.563323
0.5	0.5	0.5	1	0.5	0.1	1	0.1	1	0.4	1	0.1	1.597692
0.5	0.5	0.5	1	0.5	0.1	2	0.1	1	0.4	1	0.1	1.666429
0.5	0.5	0.5	1	0.5	0.1	0.1	0	1	0.4	1	0.1	1.528955
0.5	0.5	0.5	1	0.5	0.1	0.1	1.5	1	0.4	1	0.1	1.563323
0.5	0.5	0.5	1	0.5	0.1	0.1	1	1	0.4	1	0.1	1.597692
0.5	0.5	0.5	1	0.5	0.1	0.1	2	1	0.4	1	0.1	1.666429
0.5	0.5	0.5	1	0.5	0.1	0.1	0.1	1	0.4	1	0.1	0.193061
0.5	0.5	0.5	1	0.5	0.1	0.1	0.1	2	0.4	1	0.1	0.192503
0.5	0.5	0.5	1	0.5	0.1	0.1	0.1	5	0.4	1	0.1	0.192014
0.5	0.5	0.5	1	0.5	0.1	0.1	0.1	10	0.4	1	0.1	0.192014
0.5	0.5	0.5	1	0.5	0.1	0.1	0.1	1	0	2	0.1	0.078848
0.5	0.5	0.5	1	0.5	0.1	0.1	0.1	1	0.5	2	0.1	0.092764
0.5	0.5	0.5	1	0.5	0.1	0.1	0.1	1	0.75	2	0.1	0.094474
0.5	0.5	0.5	1	0.5	0.1	0.1	0.1	1	1	2	0.1	0.095398
0.5	0.5	0.5	1	0.5	0.1	0.1	0.1	1	0.4	1.5	0.1	0.084362
0.5	0.5	0.5	1	0.5	0.1	0.1	0.1	1	0.4	2	0.1	0.091647
0.5	0.5	0.5	1	0.5	0.1	0.1	0.1	1	0.4	2.5	0.1	0.094432
0.5	0.5	0.5	1	0.5	0.1	0.1	0.1	1	0.4	3	0.1	0.095892
0.5	0.5	0.5	1	0.5	0.1	0.1	0.1	1	0.4	1	0	0.000000
0.5	0.5	0.5	1	0.5	0.1	0.1	0.1	1	0.4	1	0.5	1.427927
0.5	0.5	0.5	1	0.5	0.1	0.1	0.1	1	0.4	1	0.75	3.060111
0.5	0.5	0.5	1	0.5	0.1	0.1	0.1	1	0.4	1	1	7.141826

Table 4 Numerical results for and local Sherwood number $-\phi'(0)$ for M, β, K, Sc, Kr, λ and f_w with Pr = 2, Q = 0.5, Ec = 0.1, Ec_x = 0.1, Ec_y = 0.1 & Bi = 0.1.

M	β	K	Sc	Kr	λ	f_w	$-\phi'(0)$
0.5	0.5	0.5	1	0.3	0.4	1	1.681559
1	0.5	0.5	1	0.3	0.4	1	1.718016
1.5	0.5	0.5	1	0.3	0.4	1	1.745905
2	0.5	0.5	1	0.3	0.4	1	1.768350
0.5	1	0.5	1	0.3	0.4	1	1.796355
0.5	1.5	0.5	1	0.3	0.4	1	1.841491
0.5	2	0.5	1	0.3	0.4	1	1.865870
0.5	0.5	1	1	0.3	0.4	1	1.543299
0.5	0.5	1.5	1	0.3	0.4	1	1.430854
0.5	0.5	2	1	0.3	0.4	1	1.320613
0.5	0.5	0.5	1	0.3	0.4	1	1.681559
0.5	0.5	0.5	2	0.3	0.4	1	3.548308
0.5	0.5	0.5	5	0.3	0.4	1	9.479678
0.5	0.5	0.5	10	0.3	0.4	1	19.467263
0.5	0.5	0.5	1	0.5	0.4	1	1.820140
0.5	0.5	0.5	1	1	0.4	1	2.089278
0.5	0.5	0.5	1	2	0.4	1	2.484232
0.5	0.5	0.5	1	0.3	0	1	1.363739
0.5	0.5	0.5	1	0.3	0.5	1	1.726567
0.5	0.5	0.5	1	0.3	0.75	1	1.808987
0.5	0.5	0.5	1	0.3	1	1	1.864560
0.5	0.5	0.5	1	0.3	0.4	0	2.794205
0.5	0.5	0.5	1	0.3	0.4	2	3.857938
0.5	0.5	0.5	1	0.3	0.4	2.5	4.896404
0.5	0.5	0.5	1	0.3	0.4	3	5.921597

References

[1] Ahmed M.Megahed, (2015), MHD viscous Casson fluid flow and heat transfer with second-order slip velocity and thermal slip over a permeable stretching sheet in the presence of internal heat generation/absorption and thermal radiation, The European Physical Journal Plus, Vol.130:81

[2] Anwar, M. I., Khan, I.,Sharidan, S., and Salleh, M. Z., (2012), Conjugate effects of heat and mass transfer ofnanofluids over a nonlinear stretching sheet, International Journal of Physical Sciences, Vol. 7(26), pp. 4081 - 4092.

[3] Bhargava, R., Sharma, S., Takhar, H.S., Beg, O.A., and Bhargava, P., (2007), Numerical solutions for micropolar transport phenomena over a nonlinear stretching sheet, Nonlinear Anal. Model. Cont., Vol.12, pp.45-63.

[4] ChennaSumalatha, Shankar Bandari, (2015), Effects of Radiations and Heat Source/Sink on a Casson Fluid Flow over Nonlinear Stretching Sheet, World Journal of Mechanics, Vol.5, pp.257-265.

[5] El-Dabe N.T., Ghaly A.Y., Rizkallah R.R., Ewis,K.M. and Al-Bareda.A.S., (2015), Numerical solution of MHD boundary layer flow of Non-Newtonian Casson Fluid on a moving wedge with Heat and mass transfer and Induced Magnetic Field, Journal of Applied Mathematics and Physics, Vol.3, pp.649-663.

[6]   Eldabe, N.T.M. and Salwa, M.G.E., (1995), Heat Transfer of MHD Non-Newtonian Casson Fluid Flow between Two Rotating Cylinders, Journal of the Physical Society of Japan, Vol.64, 41.
[7]   Gireesha B.J., Rama Subba Reddy Gorla, and Mahanthesh B., (2015), Effect of Suspended Nanoparticles on Three-Dimensional MHD Flow, Heat and Mass Transfer of Radiating Eyring-Powell Fluid Over a Stretching Sheet, Journal of Nanofluids, Vol.4, pp.1-11.
[8]   Hayat, T., and Qasim, M., (2011), Radiation and magnetic field effects on the unsteady mixed convection flow of a second grade fluid over a vertical stretching sheet, Int. J. Numer. Meth. Fluids, Vol.66, pp.820-832.
[9]   Hyat T., Awais. M., Asghar. S., (2013), Radiative effects in a three-dimensional flow of MHD Eyring-Powell fluid, Journal of the Egyptian Mathematical Society, Vol.21, Issue 3, pp.379-384.
[10]   Jat R.N. and Anju K. Jhanka, (2003), Three-dimensional free convective MHD flow and heat transfer through a porous medium, Indian Journal of Engineering and Materials sciences, Vol.10, pp.138-142.
[11]   Kar M., Dash G.C., Sahoo S.N., Rath P.K., (2013),Three-Dimensional free convection MHD flow in a vertical channel through a porous medium with heat source and chemical reaction, Journal of Engineering Thermodynamics,Vol.22,Issue 3,pp 203-215.
[12]   Khan, W. A. and Pop, I., (2010), Boundary-layer flow of a nanofluid past a stretching sheet, International Journal of Heat and MassTransfer, Vol. 53, No. 11-12, pp. 2477-2483.
[13]   Mustafa Turkyilmazoglu, (2012), Three Dimensional MHD stagnation flow due to a stretchable rotating disk, International Journal of Heat and Mass Transfer, Vol.55, Issue 23-24, pp.6959-6965.
[14]   Pal, D., and Mondal, H., (2010), Soret and Dufour effects on MHD non-Darcian mixed convection heat and mass transfer over a stretching sheet with non-uniform heat source/sink, Physica B., Vol.85, pp.941-951.
[15]   Peri K kameswaran, Shaw S., Sibanda P., (2014), Dual solutions of Casson fluid over a stretching or shrinking sheet, Springer India, Vol.39, pp.1573-1583.
[16]   Pramanik S., (2014), Casson fluid flow and heat transfer past an exponentially porous stretching surface in presence of thermal radiation, Ain Shams Engineering Journal, Vol.5, pp.205-212.
[17]   Rajagopal K., Veena P.H., Pravin V.K., (2013), Unsteady Three-Dimensional MHD Flow Due to Impulsive Motion with Heat and Mass transfer Past a Stretching Sheet in a Saturated Porous Medium, International Journal of Applied Mechanics and Engineering, Volo.18, Issue 1, pp.137-151.
[18]   Raju C.S.K.., Sandeep N., JayachandraBabu M., Sugunamma V., (2016),Dual solutions for three-0.dimensional MHD flow of a nanoluid over a nonlinearly permeable stretching sheet, Alexandria Engineering Journal, Vol.55, pp.151-162.
[19]   Ramzan M., (2015), Influence of Newtonian Heating on Three-Dimensional MHD Flow of Couple Stress Nanofluid with Viscous dissipation and Joule heating, PLos ONE 10(4) eo 124699,doi:1371/journal,phone.0124699.
[20]   Sarojamma G., Venda bai K., (2015), Boundary Layer Flow of a Cassonnanofluid past a vertical exponentially Stretching Cylinder in the Presence of a Transfer Magnetic Field with Internal Heat Generation/Absorption, World Academy of science, Engineering and Technology International Journal of Mechanical, Aerospace, Industrial, Mechatronic and Manufacturing Engineering, Vol.9, No.1, pp.138-143.
[21]   Shampine, L. F. and Kierzenka, J. (2000), "Solving boundary value problems for ordinary differential equations in MATLAB with bvp4c," Tutorial Notes.
[22]   Srinivasacharya D., MenduUpendar, (2013), Effect of double stratification on MHD free convection in a micropolar fluid, Journal of the Egyptian Mathematical Society, Vol.21, pp.370–378.
[23]   TasawarHayata and Muhammad Nawaz, (2010), Magneto Hydrodynamic Three-Dimensional Flow of a Second –Grade Fluid with Heat Transfer, Z.Naturforch,Vol.65a, pp.683-691.